RSC Advances

ROYAL SOCIETY OF CHEMISTRY

www.rsc.org/advances

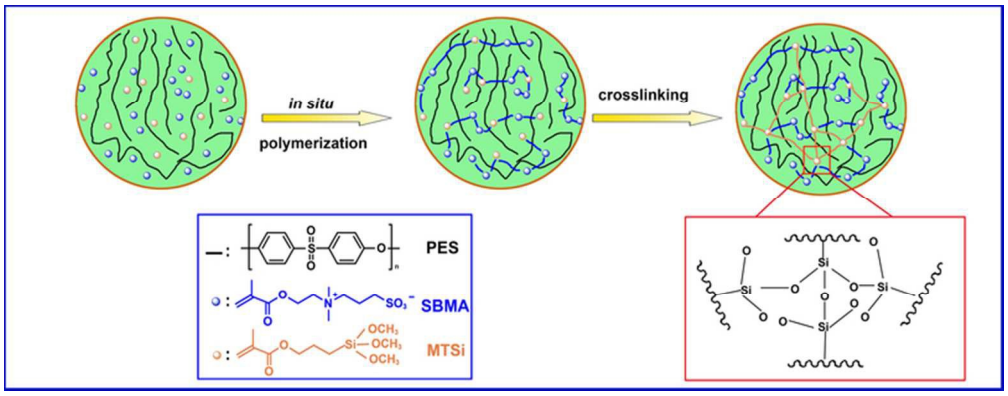

34x13mm (600 x 600 DPI)

Journal Name

RSCPublishing

ARTICLE

Improved antifouling property and blood compatibility of 3-methacryloxypropyl trimethoxysilane - based zwitterionic copolymer modified composite membranes via in situ post-crosslinking copolymerization

Cite this: DOI: 10.1039/x0xx00000x

Received 00th January 2012,
Accepted 00th January 2012

DOI: 10.1039/x0xx00000x

www.rsc.org/

Tao Xiang[a], Ting Lu[a], Rui Wang[a], Cheng Wang[a], Shu-Dong Sun[a], Hong-Bo He[b,*], Chang-Sheng Zhao[a,c,**]

In the present study, a new method to prepare stable antifouling and blood compatible membranes is developed, i.e., *in situ* post-crosslinking copolymerization. Firstly, 3-methacryloxypropyl trimethoxysilane (MTSi)-based zwitterionic copolymer was synthesized by *in situ* copolymerization in polyethersulfone (PES) solution and fabricated into membranes by a liquid-liquid phase separation technique. Then the membranes were treated by basic solutions to promote the crosslinking of the copolymer via the hydrolysis of the methoxy groups. The surface free energy of the poly(3-methacryloxypropyl trimethoxysilane) (PMTSi) modified membranes reduced from 55.29 to 43.91 nJ/cm^2. For the poly(3-methacryloxypropyl trimethoxysilane-*co*-sulfobetaine methacrylate) (P(MTSi-*co*-SBMA)) modified membranes, the hydrolyzed PMTSi segments were used as the crosslinker to make the membrane stable. Both the PMTSi and P(MTSi-*co*-SBMA) modified membranes showed improved antifouling property and blood compatibility (lowered protein adsorption amount, suppressed platelet adhesion and prolonged clotting time) compared with the pristine PES membrane. Thus the modified membranes provided wide choice for specific biomedical applications.

Introduction

Fouling is a severe problem for the press-driven membranes, such as microfiltration (MF) membrane, ultrafiltration (UF) membrane, nanofiltration (NF) membrane and reverse osmosis (RO) membrane, hampering the application of the membranes in water treatment, pharmaceuticals and biochemical industries.[1-7] The fouling is usually caused by the interaction between the membrane surface and the foulants, including organic, biological substances in many forms. It not only decreases the permeability performance and membrane life, but also increases the overall energy requirement. Thus, membrane fouling has been a subject of many academic studies and industrial research efforts.[1]

To control and decrease membrane fouling, many efforts have been paid to introduce hydrophilic polymers into the membranes, such as poly(acrylic acid) (PAA),[8] poly(N-vinylpyrrolidone) (PVP),[9] polyethylene glycol (PEG) and its derivatives,[10-13] as well as zwitterionic polymers.[14-19] Among the above polymers, zwitterionic polymers containing the pendant groups of phosphobetaine, sulfobetaine or carboxybetaine are especially effective to improve the antifouling property for different materials. The zwitterionic polymers have both a positively and negatively charged moieties within the same segment side chain, and maintain overall charge neutrality.[20] Both experimental and theoretical studies have suggested that the antifouling property of zwitterionic betaines stemmed from the opposite charges being highly hydrated.[21, 22]

In recent years, many methods have been utilized to introduce zwitterionic polymers into materials, including blending method,[23, 24] surface-initiated ATRP,[18, 25-27] click chemistry-enabled layer-by-layer (LBL)[14] and so on. Among these methods, blending is the simplest but most important method to prepare modified materials; however, the elution of the hydrophilic functional polymers is unavoidable. In our recent studies,[28-32] many amphiphilic copolymers were synthesized to modify polyethersulfone (PES) membranes with pH-sensitivity and antifouling property, for which hydrophobic monomers such as methyl methacrylate (MMA), styrene (St) and acrylonitrile (AN) were copolymerized to decrease the copolymer elution. However, the elution was hardly avoided and the miscibility of the copolymers and PES in the common solvent was poor. Recently, we reported a new method, namely *in situ* cross-linked polymerization/copolymerization to prepare functional

membranes.[33-35] The semi-interpenetrating network (semi-IPN) structure endowed the membranes with stable structure and nearly no elution during use. The problem is that the cross-linked structure limits the surface enrichment of the hydrophilic polymer. Thus, we propose a new method, namely *in situ* post-crosslinking copolymerization to prepare modified membranes. A multifunctional compound of 3-methacryloxypropyl trimethoxysilane (MTSi), possessing both vinyl groups and methoxy groups,[36, 37] can be used as the monomer in the radical polymerization and the cross-linker in the post-processing.

In this study, we proposed a new method, i.e., *in situ* post-crosslinking copolymerization to prepare modified membranes with improved antifouling property and blood compatibility. A zwitterionic copolymer of poly(3-methacryloxypropyl trimethoxysilane-*co*-sulfobetaine methacrylate) (P(MTSi-*co*-SBMA)) was firstly synthesized in PES solution and then fabricated into membranes. The membranes were then crosslinked *via* the hydrolysis of the methoxy groups. Three kinds of post-crosslinking methods were applied to increase the surface enrichment of hydrophilic polymer in the post-crosslinking process. The ultrafiltration experiments for pure water and BSA solution were used to investigate the permeability and antifouling property. The blood compatibility including protein adsorption, platelet adhesion, activated partial thromboplastin time (APTT) and thrombin time (TT)) of the modified membranes was also evaluated.

Materials and methods

Materials

Polyethersulfone (PES, Ultrason E6020P, Mw=51000 g/mol) was purchased from BASF. Sulfobetaine methacrylate (SBMA) was synthesized using 2-(dimethylamino) ethyl methacrylate (DMAEMA, 99%, Aladdin) and 1,3-propanesulfonate (99%, Aladdin) as the reagents.[18] 2, 2'-Azobis(2-methylpropionitrile) (AIBN, 98%, Aladdin) was purified by recrystallization. Dimethyl sulfoxide (DMSO, 99.8%, Aladdin) was vacuum distilled before use. 3-Methacryloxypropyl trimethoxysilane (MTSi, 97%, Aladdin), N,N'-methylenebisacrylamide (MBA, 99%, Aladdin) and triethylamine (TEA, 99%, Aladdin) were used as received. Bovine serum albumin (BSA, fraction V, ≥95%) and bovine serum fibrinogen (BFG, ≥75%) were obtained from Sigma Chemical Co. Micro BCA™ protein assay reagent kits were the products of PIERCE. APTT and TT reagent kits were purchased from SIEMENS. Ultrapure water was used throughout the studies.

Membrane preparation

In this study, poly(3-methacryloxypropyl trimethoxysilane) (PMTSi) and poly(3-methacryloxypropyl trimethoxysilane-*co*-sulfobetaine methacrylate) (P(MTSi-*co*-SBMA)) modified membranes were prepared by three steps as shown in Scheme 1. Firstly, PMTSi and P(MTSi-*co*-SBMA) polymers were synthesized in PES solution via *in situ* free radical polymerization/copolymerization initiated by AIBN. Secondly, the obtained solutions were directly fabricated into membranes by spin casting coupled with a liquid-liquid phase separation technique after being vacuum degassed.[38] Finally, the PMTSi and P(MTSi-*co*-SBMA) polymers in the membranes were crosslinked by the hydrolysis of the methoxy groups under basic condition (2 volume% TEA) at 60 °C.

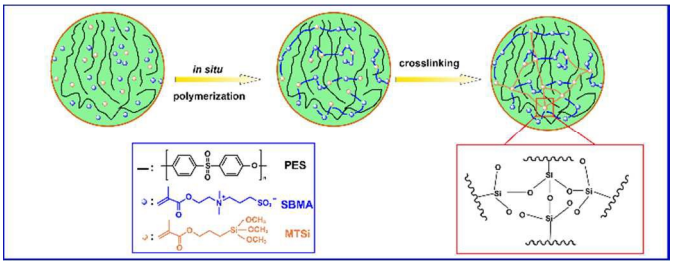

Scheme 1. Scheme illustration for the preparation of PMTSi and P(MTSi-*co*-SBMA) modified membranes by the *in situ* post-crosslinking copolymerization.

A typical procedure for the synthesis of PMTSi and P(MTSi-*co*-SBMA) polymers in PES solution was as follows: the total weight of the reaction system was 100 g. 16 g PES (16 *wt.*% of the total solution) was firstly dissolved in 60 g DMSO to get a homogeneous solution. Then the mixture of SBMA, MTSi, AIBN and MBA dissolved in DMSO was added into the PES solution under nitrogen atmosphere. The polymerization was carried out at 75 °C with vigorous stirring for 24 h. After that, the reaction solution was cooled to room temperature and vacuum degassed. The reaction solution was then prepared into membranes by spin casting coupled with a liquid-liquid phase separation technique at room temperature. The membranes were rinsed with deionized water thoroughly to remove the residual solvent. All the prepared membranes were in a uniform thickness of about 60 ± 3 μm. Then, the PMTSi and P(MTSi-*co*-SBMA) in the membranes were crosslinked by the hydrolysis of the methoxy groups under basic condition *via* three different methods as shown in Table 1. The membranes were then washed and stored in ultrapure water before use.

Table 1. The compositions and post-crosslinking methods for the modified membranes prepared by the *in situ* post-crosslinking polymerization.

Membrane No.	PES (g)	MTSi (g)	SBMA (g)	AIBN (mol%)	MBA (mol %)	post-crosslinking method[a]
M-Si-1	16	2	0	2	2	method 1
M-Si-2	16	2	0	2	2	method 2
M-Si-3	16	2	0	2	2	method 3
M-Si/PSBMA-1	16	2	3	2	2	method 1
M-Si/PSBMA-2	16	2	3	2	2	method 2
M-Si/PSBMA-3	16	2	3	2	2	method 3

[a] post-crosslinking method. Method 1: basic aqueous solution at 60 °C for 5 h. Method 2: basic alcohol solution at 60 °C for 5 h. Method 3: basic alcohol solution at 60 °C for 5 h and then basic aqueous solution at 60 °C for 5 h.

Characterization

Thermogravimetric analysis (TG) was performed using a TG209F1 TG instrument (Netzsch, Germany) at a heating rate of 10 °C/min and N_2 atmosphere. Differential Scanning Calorimetry (DSC) measurements were conducted on a computer control electronic universal testing machine Q2000 (TA, America) and scanned from -50 and 300 °C at a heating rate of 5 °C/min and N_2 atmosphere. Fourier transform infrared (FTIR) spectra were obtained by Nicolet 560 (Nicolet Co., American) instrument; and each spectrum was collected at a resolution of 4 cm^{-1} and the reflectance spectra were scanned over the range of 500-4000 cm^{-1}. To prepare FTIR sample, the membrane was dissolved in DMSO and cast on a potassium bromide (KBr) disc with the thickness of about 0.8 mm, and then the cast polymer solution was dried by an infrared light.

The cross-section morphologies of the membranes were characterized by using JSM-7500F field-emission scanning microscope (SEM) (JEOL, Japan) with the voltage of 5 kV. The elemental compositions of membrane surfaces were confirmed by SEM-EDS using EDS accessory and a Kratos AXIS ULTRA^{DLD} XPS Instrument, employing Al Kαexcitation radiation .

Membrane porosity, mean pore size and water uptake

The membrane porosity was an important parameter to characterize membrane and has significant effect on membrane permeability, which was defined as the volume of the pores divided by the total volume of the porous membrane.[39, 40] The fabricated membranes were firstly withdrawn from water, and the excess surface water was removed with filter paper and the membranes were weighed. Then the membranes were dried in vacuum at 60 °C for about 48 h. At least three parallel samples were tested in the experiment.

The porosity (ε) was calculated using the following equation:

$$\varepsilon = \frac{(W_W - W_D)/\rho_W}{W_D(1-C\%)/\rho_P + W_D C\%/\rho_C + (W_W - W_D)/\rho_W} \times 100\% \quad (1)$$

where W_W is the weight of wet membranes (g); W_D is the weight of dry membranes (g); ρ_W is the density of water, ρ_W = 1.0 g/cm^3; ρ_P is the density of PES, ρ_P = 1.43 g/cm^3; ρ_C is the density of PMTSi or P(MTSi-*co*-SBMA), $\rho_C \approx$ 1.4 g/cm^3; *C%* is the mass percent of the PMTSi or P(MTSi-*co*-SBMA) in the membranes.

The mean pore size (r_m) of the membranes was calculated using Guerout-Elford-Ferry equation (Equ. (2)) on the basis of pure water flux and porosity data of the membranes:[41-43]

$$r_m = \sqrt{\frac{(2.9-1.75\varepsilon)8\eta l Q}{\varepsilon A \Delta P}} \quad (2)$$

where ε is the porosity; η is the pure water viscosity (8.9×10^{-4} Pa.S); l is the membrane thickness (m); Q is the permeation volume of pure water per unit time (m^3/s); A is the effective membrane area (13.8 cm^2); ΔP is the operation pressure (0.05 MPa).

Water uptake (WU) of the modified membranes was evaluated by comparing the weights of the dry and wet membranes. The completely dry membranes were weighed firstly and then immersed in ultrapure water at room temperature for 24 h. Then the membranes were withdrawn from water, and the excess surface water was removed with filter paper and the membranes were weighed again. The WU was calculated by the following equation:

$$WU = \frac{W_{Wet} - W_{Dry}}{W_{Dry}} \times 100\% \quad (3)$$

where W_{Wet}, W_{Dry} are the weights of the wet and dry membranes, respectively.

Contact angle and surface free energy measurement

The contact angles of water and diiodomethane were measured and calculated on a contact angle goniometer (DSA100 (KRUSS GmbH, Germany) equipped with a video capture at ambient temperature. One drop of wetting agent (3 μL) was dropped onto the surface of the membrane with an automatic piston syringe and photographed, and then contact angle was measured after 10 s. At least eight measurements were conducted to get a reliable value. The water contact angles for each membrane decaying with time (to 200 s) were also measured.

The surface free energy including the dispersion component γ_S^d and polar component γ_S^p, which were calculated from the contact angles of water and diiodomethane based on the following equation:[44]

$$\cos\theta = -1 + \frac{2\sqrt{\gamma_S^d \gamma_L^d}}{\gamma_L} + \frac{2\sqrt{\gamma_S^p \gamma_L^p}}{\gamma_L} \quad (4)$$

where θ is the measured contact angle; γ_L, γ_L^d and γ_L^p are the total surface free energy, dispersion component, and polar dispersion of the wetting reagents, respectively. The total solid-surface free energy γ_S can be expressed as:

$$\gamma_S = \gamma_S^d + \gamma_S^p \quad (5)$$

Ultrafiltration experiments

Ultrafiltration experiments were conducted using the apparatus as described in our previous study.[8] A dead-end ultrafiltration (UF) cell with an effective membrane area of 13.8 cm^2 was used. Before the ultrafiltration experiments, the membranes were pre-compacted with deionized water for 30 min at a pressure of 0.1 MPa to get steady filtration (with a flux difference lower than 2% in periods of 5 min). All the ultrafiltration experiments were operated at a pressure of 0.05 MP at room temperature. The water flux was determined as follows:

$$Flux = \frac{V}{SPt} \quad (6)$$

where V (mL) is the volume of the permeated solution; S (m^2) is the effective membrane area; P (mmHg) is the pressure applied to the membrane and t (h) is the time for collecting permeated solution.

For the ultrafiltration of bovine serum albumin (BSA), the filtration cell was emptied and refilled with BSA solution, in which BSA was dissolved in isotonic phosphate-buffered saline solution (PBS, pH 7.4) with a concentration of 1.0 mg/mL. The flux was calculated by Eq. (6) and the protein rejection ratio (R) was calculated by the following equation:

$$R = (1 - \frac{C_p}{C_f}) \times 100\% \quad (7)$$

where C_p and C_f (mg/mL) are the protein concentrations of the permeate and feed solutions, respectively. The protein concentration was measured by an UV-vis spectrophotometer (UV-1750, Shimadzu, Japan) at the wavelength of 278 nm.

After protein filtration, the membrane was cleaned with deionized water; then, the PBS flux of the cleaned membrane was measured again. The flux recovery ratio (F_{RR}) was calculated using the following equation:

$$F_{RR} = (\frac{F_2}{F_1}) \times 100\% \quad (8)$$

where F_1 and F_2 (mL/m^2·h·mmHg) are the PBS fluxes before and after protein ultrafiltration, respectively.

Blood compatibility

Plasma collection

Healthy human fresh blood (man, 25 years old) was collected using vacuum tubes (5 mL, Terumo Co.), containing citrate/phosphate/dextrose/adenine-1 mixture solution (CPDA-1) as the anticoagulant (anticoagulant to blood ratio, 1:9). The blood was centrifuged at 1000 rpm (or 4000 rpm) for 15 min to obtain platelet-rich plasma (PRP) (or platelet-poor plasma (PPP)). All the blood compatibility experiments were performed in compliance with the relevant laws and institutional guidelines.

Protein adsorption

BSA and BFG were used in protein adsorption experiments. The protein (BSA or BFG) was dissolved in isotonic phosphate-buffered saline solution (PBS, pH 7.4) with a concentration of 1 mg/mL. The membrane with an area of 1 × 1 cm^2 was incubated in PBS at 4 °C for 24 h and equilibrated at 37 °C for 1 h, and then immersed in the protein solution at 37 °C for 2 h. After protein adsorption, the membrane was gently rinsed with PBS and then immersed in 2 *wt.*% aqueous sodium dodecyl sulfate (SDS) solution at 37 °C for 1 h under agitation to remove the protein adsorbed on the membrane. The protein amount in the SDS solution was quantified by Micro BCA^{TM} protein assay reagent kits, and the protein concentration was measured by a UV-vis spectrophotometer (UV-1750, Shimadzu, Japan) at the wavelength of 562 nm. More than 95% of the protein

adsorbed on the membranes could be eluted into the SDS solution. Then the adsorbed protein amount was calculated.

Platelet adhesion

In order to eliminate the interference of other components in blood, such as erythrocytes and leucocytes, platelet-rich-plasma (PRP) was used for platelet adhesion experiment. The test procedure was as follows: the membrane with an area of 1 × 1 cm^2 was incubated in PBS at 4 °C for 24 h and equilibrated at 37 °C for 1 h. Then the PBS was removed and 1 mL of fresh PRP was introduced and the membrane was incubated with PRP at 37 °C for 2 h. Then the PRP was removed and the membrane was rinsed three times with PBS, and the membrane was treated with 2.5 *wt.*% glutaraldehyde in PBS at 4 °C for at least 1 day for curing the platelets. To observe the morphology of the platelets on the surface, the membrane was washed with PBS, and subjected to a drying process by immersing in a series of graded alcohol-PBS solutions (25%, 50%, 70%, 75%, 90%, 95% and 100%) and isoamyl acetate-alcohol solutions (25%, 50%, 75% and 100%) for 15 min each time. The critical point drying of the specimens was done with liquid CO_2. The number of the adherent platelets on the membrane was calculated according to five SEM images at 1000 × magnification from different places on the same membrane.

APTT and TT

Activated partial thromboplastin time (APTT) and thrombin time (TT) were used to evaluate the antithrombogenicity of the membranes, which were measured by an automated blood coagulation analyzer (CA-50, Sysmex Co., Japan). The APTT was measured as follows: the membrane with an area of 0.5 × 0.5 cm^2 (4 pieces) was incubated in PBS at 4 °C for 24 h and equilibrated at 37 °C for 1 h, then the PBS was removed and 100 μL of fresh PPP was introduced. After incubating at 37 ºC for 30 min, 50 μL of the incubated PPP was added into a test cup, followed by the addition of 50 μL APTT agent (incubated 10 min before use). After incubating at 37 °C for 3 min, 50 μL of 25 mM $CaCl_2$ solution was added, and then the APTT was measured. At least three measurements were averaged to get a reliable value. For the TT test, 100 μL of TT agent was added into the test cup (containing 50 μL of the incubated PPP), and then the TT was measured.

Results and Discussion

Chemical compositions of the membranes

In this study, the zwitterionic copolymer of P(MTSi-*co*-SBMA) was synthesized by the copolymerization of the SBMA and MTSi in PES solution. Because of being not crosslinked, the copolymer could enrich on the membrane surface. Then the copolymer modified membrane was crosslinked by the hydrolysis of the methoxy groups under basic condition.

The membranes were firstly characterized by TGA and FTIR. The TGA results are shown in Fig. 1. For all the membranes, the weight loss below 120 ºC was due to the desorption of adsorbed water. For the M-0 membrane, in the range of 120-800 °C, the weight loss of M-0 was 58.2%, which was ascribed to the decomposition of PES. For the M-Si-1~3 and M-Si/PSBMA-1~3 membranes, the weight losses were about 61.7% and 66.6%, respectively. The increase of weight loss indicated that the MTSi and SBMA were successfully copolymerized in the reaction. Fig. 1 (a) also showed that the membranes with the same content of zwitterionic copolymer treated with different methods possessed almost the same TG curves for both M-Si-1~3 and M-Si/PSBMA-1~3 membranes. As showed in Fig. 1 (b), for the M-0 membrane, a peak at 538 °C in the derivative thermogravimetry (DTG) curve was observed. For the M-Si-1 membrane, only one peak at 586 °C for the decomposition of PES and PMTSi was observed. For the M-Si/PSBMA-1 membrane, three peaks at 312, 433 and 576 °C were observed, indicating that the SBMA was successfully polymerized in the reaction.

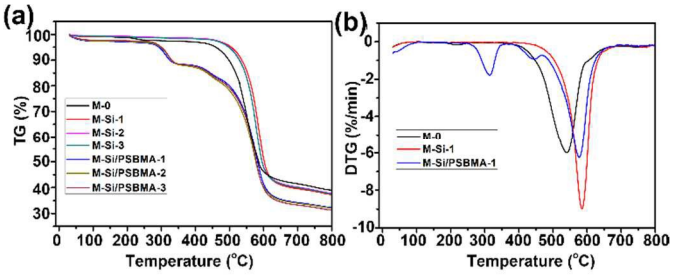

Figure 1. Thermogravimetry (TG) and derivative thermogravimetry (DTG) curves for M-0, M-Si-1~3 and M-Si/PSBMA-1~3 membranes.

The chemical compositions of the membranes were then confirmed by FTIR as shown in Fig. 2. The membranes were dissolved in DMSO and cast on a potassium bromide (KBr) disc. After the samples were dried by an infrared light, FTIR spectra were obtained. Compared with the M-0 membrane, a new band at 1724.1 cm^{-1} was observed for the M-Si-1 and M-Si/PSBMA-1 membranes, which was attributed to the ester groups (O-C=O) in MTSi and SBMA. Simultaneously, the band intensity for the M-Si/PSBMA-1 membrane was stronger than that of the M-Si-1 membrane due to the larger amount of the ester groups. The TGA and FTIR results indicated that the P(MTSi-*co*-SBMA) copolymer was successfully synthesized, and the membranes crosslinked by different methods shared the same chemical compositions.

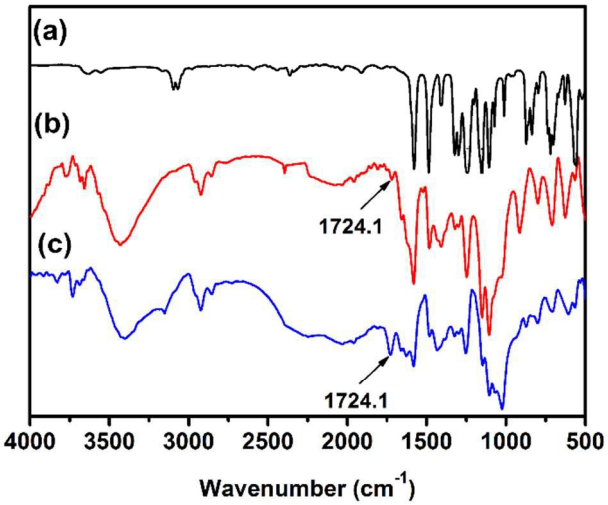

Figure 2. FTIR spectra for the M-0 (a), M-Si-1 (b) and M-Si/PSBMA-1 (c) membranes.

Morphologies and surface chemical compositions of membranes

The SEM images of the cross-section views for the membranes M-0, M-Si-1~3 and M-Si/PSBMA-1~3 are shown in Fig. 3. For the membrane M-0, spongy structure was observed and the structure was evenly distributed in the cross-section. The images of PES membrane (DMSO as the solvent) were different from those of the PES membranes prepared using dimethylacetamide (DMAc) and N-methyl pyrrolidone (NMP) as the solvents,[8, 45] for which there was a skin layer, and followed was a finger-like structure. For the M-Si-1~3 membranes, large amount of regular macrovoids were observed, which were resulted from the effect of PMTSi on the liquid-liquid phase separation process. For the M-Si/PSBMA-1~3 membranes, the amphiphilic P(MTSi-*co*-SBMA) copolymers were synthesized and the macrovoids in the cross-section were irregular. It was also found that though different post-crosslinking methods were used, the cross-

section structures were similar for the M-Si and M-Si/PSBMA membranes.

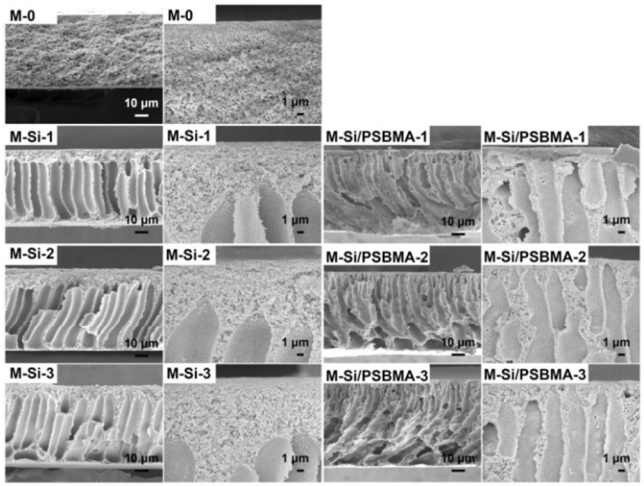

Figure 3. SEM images of the cross-section views of M-Si-1~3 and M-Si/PSBMA-1~3 membranes.

SEM-EDS was adopted to quantitatively analyze the surface chemical compositions, as shown in Table 2. The data showed that for the M-Si-1~3 and M-Si/PSBMA-1~3 membranes treated by different post-crosslinking methods, the Si content was increased from 0.37% to 0.49% and from 0.33% to 0.45%, respectively. To further analyze the chemical compositions of the membrane surfaces, XPS was also adopted and the results were shown in Table 2 and Fig. S2. We could found that the Si content was significantly increased from 0.11% to 1.13% and the N content was increase from 0.81% to 2.18%, respectively. Thus, we could make a conclusion that the surface enrichment was enhanced from method 1 to method 3 for both M-Si-1~3 and M-Si/PSBMA-1~3 membranes. The improved enrichment was resulted from the solubility difference of the PMTSi and P(MTSi-*co*-SBMA) polymers in alcohol and water; since the polymers were dissolved in alcohol, and the treatment by basic alcohol solution led to the migration of PMTSi and P(MTSi-*co*-SBMA) polymers to the membrane surface.

Table 2. Surface elemental compositions of the membranes measured by EDS and XPS.

	Sample	Atom quantity percentage (%)				
		C	O	S	Si	N
EDS	M-0	77.85	15.93	6.22	-	-
	M-Si-1	78.22	15.44	5.97	0.37	-
	M-Si-2	77.68	16.75	5.15	0.42	-
	M-Si-3	78.74	16.45	4.32	0.49	-
	M-Si/PSBMA-1	74.38	17.94	6.8	0.33	0.55
	M-Si/PSBMA-2	73.35	18.76	6.89	0.38	0.62
	M-Si/PSBMA-3	72.62	19.12	6.94	0.45	0.87
XPS	M-0	78.41	15.97	4.21	-	-
	M-Si/PSBMA-1	75.97	18.32	4.79	0.11	0.81
	M-Si/PSBMA-2	74.01	17.89	3.54	0.54	4.02
	M-Si/PSBMA-3	73.12	19.61	3.96	1.13	2.18

Wettability and surface free energy

Contact angle measurement is widely used to characterize the hydrophilicity/ hydrophobicity of material surface, which provided wettability property of the material surface and information on the surface free energy between the surface and the liquid.[46] In this study, water and diiodomethane were used in contact angle measurement, and the results are shown in Table 3. For the M-0 membrane, the water contact angle (WCA) was 70.9° and the γ_S was 55.29 nJ/cm^2. For the M-Si-1~3 membranes, the WCAs increased from 71.3 to 82.4° and the γ_S decreased from 48.62 to 43.91 nJ/cm^2. The results indicated that the surface energy of the PMTSi modified membranes was decreased, and the surface enrichment was improved from M-Si-1 to M-Si-3. For the M-Si/PSBMA-1~3 membranes, the WCAs increased from 57.2 to 74.2° and the γ_S decreased from 61.97 to 53.36 nJ/cm^2. The results showed that the hydrophilicity was improved after introducing PSBMA into the modified membranes, and the surface enrichment was also improved.

Table 3. Contact angle and surface energy components of different membranes.

Sample	Contact angle (°)		Surface energy (nJ/cm^2)		
	Water	Diiodo methane	γ_S	γ_S^d	γ^p
M-0	70.9	20.5	55.29	44.51	10.78
M-Si-1	71.3	44.6	48.62	35.18	13.44
M-Si-2	75.5	46.5	46.83	34.32	12.51
M-Si-3	82.4	43.8	43.91	35.69	8.22
M-Si /PSBMA-1	57.2	24.1	61.97	43.24	18.42
M-Si /PSBMA-2	65.1	35.8	57.46	42.12	15.34
M-Si /PSBMA-3	74.2	20.4	53.36	40.21	13.15

Since the contact angle depends upon surface hydrophilicity (or hydrophobicity), roughness, porosity, pore size and its distribution [1], we investigated the water contact angles from 0 to 200 s as shown in Fig. 4. For all the membranes, the WCAs decreased with the time. After about 200 s, the WCAs for the modified membranes also showed increasing tendency from M-Si-1 to M-Si-3 and from M-Si/PSBMA-1 to M-Si/PSBMA-3, which were consistent with the above results.

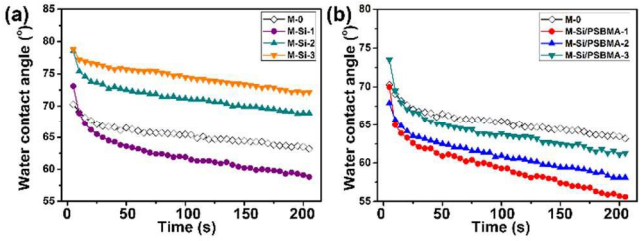

Figure 4. The water contact angles (WCAs) decaying with time for the pristine PES (M-0) and modified membranes.

Porosity, pure water flux, mean pore size and water uptake of the membranes

Porosity and mean pore size are important parameter to characterize the membrane structure as shown in Table 4. The porosity for the M-0 membrane was 79.24%. After PMTSi and P(MTSi-*co*-SBMA) were introduced, the porosities of the modified membranes decreased compared to that of the M-0 membrane. The porosity difference for the membranes with three post-linked methods was not obvious. However, the mean pore sizes for the modified membranes showed obvious changes. The M-0 owned the largest mean pore size of 18.13 nm. For the M-Si and M-Si/PSBMA membranes, the mean pore sizes were ranged from 10.66 to 15.48 nm and from 11.36 to 16.03 nm, respectively. Simultaneously, the Method 2 treated membranes owed larger mean pore size compared to the Method 1 and Method 3 treated membranes.

Table 4. Porosity, pure water flux, mean pore size and water uptake of the pristine PES and modified membranes.

Sample	Membrane porosity (%)	Pure water flux (mL/m^2·h·m mHg)	Mean pore size (nm)	Water uptake (%)
M-0	79.24	208.12	18.13	23.33
M-Si-1	77.38	67.20	10.66	94.34
M-Si-2	79.02	147.36	15.48	70.23
M-Si-3	79.04	101.21	12.67	58.56
M-Si/PSBMA-1	73.21	67.21	11.36	162.13
M-Si/PSBMA-2	75.13	147.33	16.03	87.04
M-Si/PSBMA-3	76.76	125.4	14.50	76.89

According to the studies,[41, 42] porosity and pore size had great effect on the pure water flux of membranes. As shown in Table 4, the water flux for the M-0 membrane was 208.12 mL/m^2·h·mmHg, which was larger than all the modified membrane. Since the porosities of all the membranes had little difference, the mean pore size severely affected the water flux.

To assess the hydrophilicity of the whole membranes, not just the surface hydrophilicity, water uptake was measured based on the weight change before and after the membranes were fully wetted. As shown in Table 4, the water uptake for the M-0 membrane was 23.33%. For the M-Si and M-Si/PSBMA membranes, the water uptakes were ranged from 58.56 to 94.24% and from 76.89 to 162.13%, respectively. The data indicated that the water uptakes for both the PMTSi and P(MTSi-*co*-SBMA) modified membranes were increased compared with that of the M-0 membrane, and the P(MTSi-*co*-SBMA) showed higher water uptake. What's more, though the chemical compositions and cross-section views for the M-Si-1~3 or M-Si/PSBMA-1~3 membranes were similar, the water uptakes for the Method 1 treated membranes were the largest. The reason might be that the PMTSi and P(MTSi-*co*-SBMA) of the Method 1 treated membranes were well-distributed in the membranes.

Antifouling property of membranes

To evaluate the antifouling property of the membranes, BSA is usually used as a model foulant.[2] The flux recovery ration (F_{RR}) was the characteristic parameter of the membrane antifouling property, and the higher value of F_{RR}, the better antifouling property of the membranes. The ultrafiltration results of BSA solution and PBS for three-cycle filtration are shown in Fig. 5 (a). It was observed that the flux decreased dramatically when the solution changed from PBS to BSA solution due to the fouling caused by the deposition and adsorption of protein molecules onto membrane surfaces and pore surfaces.[8] When the adsorption of protein molecules became saturated, a relatively steady flux was obtained. After the ultrafiltration of BSA solution, the membranes were washed with ultrapure water and the PBS flux was quickly increased to some extent.

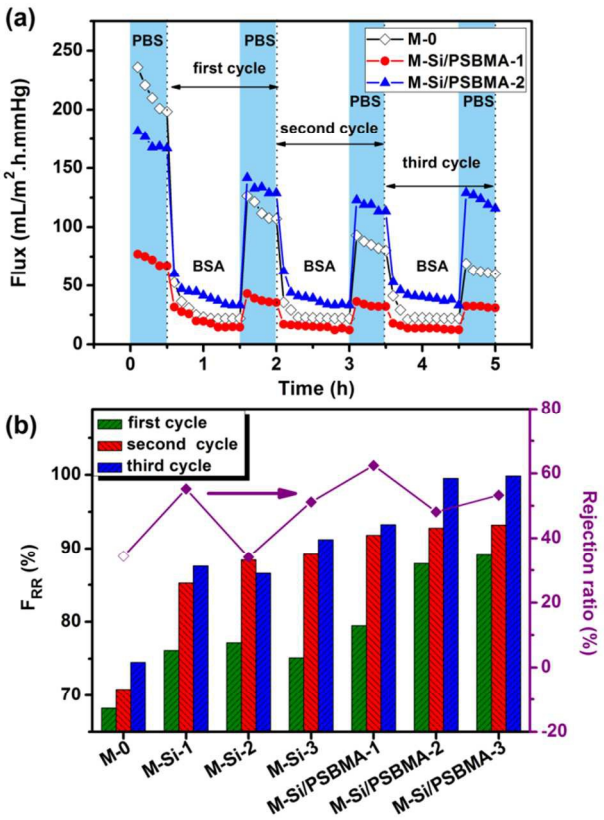

Figure 5 (a). Time-dependent fluxes of the membranes during a process of three recycles of BSA ultrafiltration at room temperature. Each recycle included ultrafiltration of BSA solution (1.0 mg/mL) and then PBS. **(b).** The flux recovery ration (F_{RR}) and rejection ration of BSA solution for the M-0 and modified membranes.

The results of F_{RR} are shown in Fig. 5 (b). For the M-0 membrane, the F_{RR}s of three cycles were 68.21%, 70.81% and 74.50%, respectively. The F_{RR}s were obviously increased for the M-Si-1~3 and M-Si/PSBMA-1~3 membranes, which were ranged from 81.58% to 86.59% and from 90.21% and 99.86%, respectively, for the three cycles. It was also found that the Method 2 and Method 3 treated membranes had higher FRRs than the Method 1 treated membranes, which might be explained by the surface enrichment. For the Method 2 and Method 3 treated membranes, surface enrichment was more efficient, resulting the more hydrophilic membrane surfaces and pores surfaces.

The results of rejection ratio are also shown in Fig. 5 (b). The rejection ratio for the M-0 membrane was about 34.23%. For the modified membranes, the rejection ratios were ranged from 34.10% to 62.45%. Comparing the data of mean pore size and rejection ratio, it was found that the membranes with larger mean pore size owned smaller rejection ratio. The phenomenon could be explained by the characterization of membrane ultrafiltration, in which the sieving of substance was realized by physical entrapment.[47]

Blood compatibility of the membranes

Protein adsorption

For blood-contacting materials, the interactions between clotting factors, plasma proteins and platelets in blood and material surfaces strongly affect the thrombotic reaction.[15, 48] Among the interactions, nonspecific protein adsorption such as fibrinogen and clotting enzymes on biomaterial surfaces is recognized as the first interaction event of many undesired bio-reactions and bio-responses, followed which were platelet adhesion and activation of coagulation

pathways, and then leading to thrombus formation.[49, 50] Thus, protein adsorption is one of the most important factors in evaluating the blood compatibility of biomaterials. In this study, BSA adsorption and BFG adsorption experiments were firstly used to measure the blood compatibility of the membranes.

Fig. 6 shows the protein adsorption results for the M-0 and modified membranes. For the M-0 membrane, the BSA adsorbed amounts were 21.9 μg/cm^2. For the M-Si-1~3 membranes, the BSA adsorbed amounts were almost the same, with the value of about 18.0 μg/cm^2. However, the BSA adsorbed amounts were obviously decreased for the M-Si/PSBMA-1~3 membranes, ranging from 8.4 to 14.8μg/cm^2. It was also found that the BSA adsorbed amounts for the M-Si/PSBMA-1~3 membranes were increased from Method 1 to Method 3 treated membranes. The results were agreed with those of the water contact angles for the M-Si/PSBMA-1~3. Similar results were found for the BFG adsorption experiment.

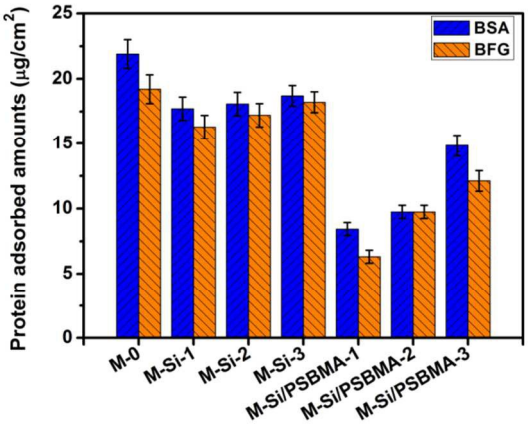

Figure 6. BSA and BFG results adsorption experiments of the PMTSi and P(MTSi-*co*-SBMA) modified membranes.

Platelet adhesion

For blood-contacting biomaterials, the adhesion and activation of platelets on the interfaces happened after protein adsorption, and were considered as key events in thrombus formation. The activated platelets can further activate many kinds of coagulation factors and then thrombus form on the surfaces.[51, 52] Therefore, *in vitro* platelet adhesion test was used to evaluate the blood compatibility of material surfaces. The morphologies and numbers of the adhered platelets could be observed on SEM images after the drying processes by series of graded alcohol-PBS solutions and isoamyl acetate-alcohol solutions.[53]

Fig. 7 shows the SEM images and the numbers of the adherent platelets on the M-0 and modified membranes. Numerous platelets aggregated and accumulated on the membrane surface (about 5.6 × 10^7 cell/cm^2), and the pseudopodia were obvious. After the PMTSi and P(MTSi-*co*-SBMA) were introduced into the membranes, the numbers of the adherent platelets were significantly decreased and fewer pseudopodia were observed. For the M-Si-1 membrane, the number of the adherent platelets was about 1.9 × 10^7 cell/cm^2 and the pseudopodia were observed. For the M-Si-2 and M-Si-3 membranes, the numbers of the adherent platelets were decreased to about 0.6 × 10^7 cell/cm^2 and the platelets expressed a rounded morphology with nearly no pseudopodia and deformation. According to the studies,[51-54] proteins especially Fibrinogen in blood plasma is particularly important for platelet adhesion since it can bind to the platelet GP IIb/IIIa receptor. Though the protein adsorbed amounts were similar for the M-Si-1~3 membranes, the M-Si-2 and M-Si-3 membranes showed fewer adherent platelets and the platelets were kept round shape with nearly no pseudopodia. These results might be resulted from the decreased surface free energy for the M-Si-2 and M-Si-3 membranes.

For the M-Si/PSBMA-1~3 membranes, the numbers of the adherent platelets were decreased from the Method 1 to Method 3 treated membranes. The results were not agreed with the protein adsorption experiments, in which the amounts of the adsorbed proteins were increased from the Method 1 to Method 3 treated membranes. Compared with the platelet adhesion results of the M-Si-1~3 membranes, it was found that the decreased surface free energy also had influence on decreasing the platelet adhesion of the M-Si/PSBMA-1~3 membranes.

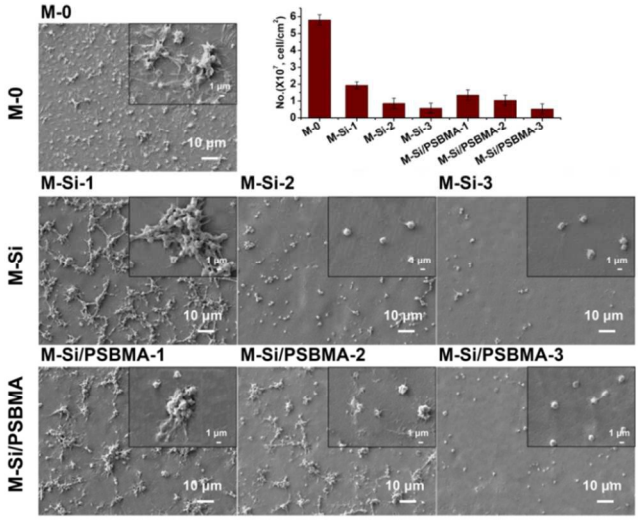

Figure 7. SEM images of the adhered platelets onto the membrane surfaces. The inserted column graph is the numbers of the adhered platelets estimated by SEM images.

Clotting time

APTT and TT tests are widely used for the clinical detection of the abnormality of the blood plasma and for the primary screening of the anticoagulative chemicals.[55] In this study, APTT and TT tests are used to assess the *in vitro* antithrombogenicity of blood-contacting materials. For the M-0 membrane, the APTT was 52.8 s. The APTT for the M-Si-1~3 and M-Si/PSBMA-1~3 membranes were about 47 s and 64 s, and little difference were found for the three post-crosslined methods. The results showed that the M-Si-1~3 could not prolong the APTT, but the M-Si/PSBMA-1~3 membranes could obviously prolong the APTT, which were consistent with the results of protein adsorption experiments.

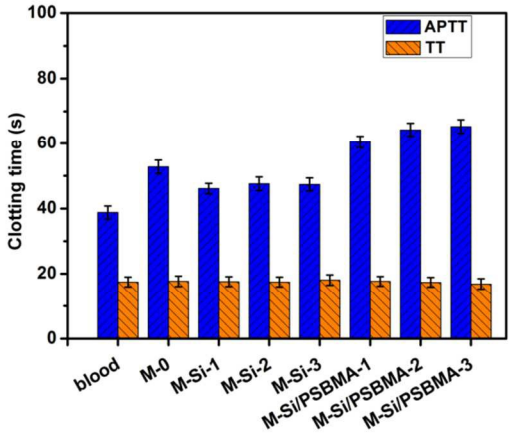

Figure 8. Activated partial thromboplastin times (APTTs) and thrombin times (TTs) for the PMTSi and P(MTSi-*co*-SBMA) modified membranes. Values are expressed as means ± SD, n=3.

However, the TTs for all the membranes were almost the same

(about 18 s). The phenomenon was also found in our previous studies.[9, 14, 18] According to the studies,[56, 57] the length of APTT reflects the level of prothrombin, fibrinogen and blood coagulation factors (V and X) in plasma in endogenous pathway of coagulation, while the length of TT reflects the level of common pathway of coagulation. Thus, the P(SBMA-*b*-NaSS) and P(SBMA-*co*-NaSS) modified membranes had effect on endogenous pathway of coagulation, attributing to the reaction or combination between the coagulation factors (V and X) in plasma and the hydrophilic surfaces.

Conclusion

Antifouling and blood compatible composite membranes were modified by the zwitterionic copolymer of poly(3-methacryloxypropyl trimethoxysilane-*co*-sulfobetaine methacrylate) (P(MTSi-*co*-SBMA)) via *in situ* post-crosslinking copolymerization. The surface enrichment of the copolymer could be adjusted by different post-linked methods. The mean pore size, porosity, water uptake and permeability for the different post-processed membranes were systematically studied. The results showed that the membranes (M-Si-1 and M-Si/PSBMA-1) treated with basic aqueous solution (method 1) owned the largest water uptake, and the membranes (M-Si-2 and M-Si/PSBMA-2) treated with basic alcohol solution (method 2) possessed the largest mean pore size and pure water flux. The antifouling property of the modified membranes was obviously improved, with the values of the flux recovery ratio (F_{RR}) above 90% for the M-Si/PSBMA membranes. The modified membranes also showed suppressed platelet adhesion, for which the decreased surface free energy had positive influence. Moreover, the clotting time was also prolonged for the M-Si/PSBMA membranes. Thus, the MTSi-based zwitterionic copolymer modified membranes with integrated antifouling property and blood compatibility had potential to be used in biomedical fields for blood purification such as hemodialysis, hemofiltration, plasma separation, and so on.

Acknowledgements

This work was financially sponsored by the National Natural Science Foundation of China (Nos. 51225303 and 51433007). We would also thank our laboratory members for their generous help, and gratefully acknowledge the help of Ms. H. Wang and S.L. Liu, of the Analytical and Testing Center at Sichuan University, for SEM observation and XPS test.

Notes and references

[a]College of Polymer Science and Engineering, State Key Laboratory of Polymer Materials Engineering, Sichuan University, Chengdu 610065, China
[b]West China Hospital, Sichuan University, Chengdu 610041, China
[c]National Engineering Research Center for Biomaterials, Sichuan University, Chengdu 610064, China
E-mail address: hxhehongbo@hotmail.com (*) or zhaochsh70@163.com (**)
Tel.: +86-28-85400453; Fax: +86-28-85405402.

1. D. Rana and T. Matsuura, *Chem. Rev.*, 2010, **110**, 2448-2471.
2. Q. Shi, J. Q. Meng, R. S. Xu, X. L. Du and Y. F. Zhang, *J. Membr. Sci.*, 2013, **144**, 50-59.
3. Y. F. Li, Y. L. Su, X. T. Zhao, R. N. Zhang, J. J. Zhao, X. C. Fan and Z. Y. Jiang, *J. Membr. Sci.*, 2014, **455**, 15-28.
4. M. Pontié, S. Rapenne, A. Thekkedath, J. Duchesne, V. Jacquemet, J. Leparc and H. Suty, *Desalination*, 2005, **181**, 75-90.
5. G. D. Kang and Y. M. Cao, *Water Res.*, 2012, **46**, 584-600.
6. R. A. Al-Juboori and T. Yusaf, *Desalination*, 2012, **302**, 1-23.
7. Y. Hoshi, Y. Xu and C. K. Ober, *Polymer*, 2013, **54**, 1762-1767.
8. L. L. Li, Z. H. Yin, F. L. Li, T. Xiang, Y. Chen and C. S. Zhao, *J. Membr. Sci.*, 2010, **349**, 56-64.
9. T. Xiang, W. W. Yue, R. Wang, S. Liang, S. D. Sun and C. S. Zhao, *Colloids Surf., B*, 2013, **110**, 15-21.
10. P. Shen, A. Moriya, S. Rajabzadeh, T. Maruyama and H. Matsuyama, *Desalination*, 2013, **325**, 37-39.
11. Q. Zhang, C. Wang, Y. Babukutty, T. Ohyama, M. Kogoma and M. Kodama, *J. Biomed. Mater. Res.*, 2002, **60**, 502-509.
12. S. J. Yuan, D. Wan, B. Liang, S. O. Pehkonen, Y. P. Ting, K. G. Neoh and E. T. Kang, *Langmuir*, 2011, **27**, 2761-2774.
13. N. Brouette and M. Sferrazza, *J. Colloid Interface Sci.*, 2013, **394**, 643-645.
14. T. Xiang, R. Wang, W. F. Zhao and C. S. Zhao, *Langmuir*, 2014, **30**, 5115-5125.
15. Y. Chang, Y. J. Shih, C. J. Lai, H. H. Kung and S. Y. Jiang, *Adv. Funct. Mater.*, 2013, **23**, 1100-1110.
16. L. Mi and S. Y. Jiang, *Biomaterials*, 2012, **33**, 8928-8933.
17. J. Zhao, Q. Shi, S. F. Luan, L. J. Song, H. W. Yang, H. C. Shi, J. Jin, X. L. Li, J. H. Yin and P. Stagnaro, *J. Membr. Sci.*, 2011, **369**, 5-12.
18. W. W. Yue, H. J. Li, T. Xiang, H. Qin, S. D. Sun and C. S. Zhao, *J. Membr. Sci.*, 2013, **446**, 79-91.
19. A. B. Lowe and C. L. McCormick, *Chem. Rev.*, 2002, **102**, 4177-4190.
20. Y. Chang, W. J. Chang, Y. J. Shih, T. C. Wei and G. H. Hsiue, *ACS Appl. Mater. Interfaces*, 2011, **3**, 1228-1237.
21. S. Chen, L. Li, C. Zhao and J. Zheng, *Polymer*, 2010, **51**, 5283-5293.
22. J. Wu, W. Lin, Z. Wang, S. Chen and Y. Chang, *Langmuir*, 2012, **28**, 7436-7441.
23. Q. Sun, Y. L. Su, X. L. Ma, Y. Q. Wang and Z. Y. Jiang, *J. Membr. Sci.*, 2006, **285**, 299-305.
24. T. Wang, Y. Q. Wang, Y. L. Su and Z. Y. Jiang, *J. Membr. Sci.*, 2006, **280**, 343-350.
25. M. Wang, J. Yuan, X. B. Huang, X. M. Cai, L. Li and J. Shen, *Colloids Surf., B*, 2013, **103**, 52-58.
26. J. Yuan, J. Q. Meng, Y. L. Kang, Q. Y. Du and Y. F. Zhang, *Appl. Surf. Sci.*, 2012, **258**, 2856-2863.
27. P. S. Liu, Q. Chen, X. Liu, B. Yuan, S. S. Wu, J. Shen and S. C. Lin, *Biomacromolecules*, 2009, **10**, 2809-2816.
28. T. Xiang, Q. H. Zhou, K. Li, L. L. Li, F. F. Su, B. S. Qian and C. S. Zhao, *Sep. Sci. Technol.*, 2010, **45**, 2017-2027.
29. T. Xiang, M. Tang, Y. Q. Liu, H. J. Li, L. L. Li, W. Y. Cao, S. D. Sun and C. S. Zhao, *Desalination*, 2012, **295**, 26-34.
30. W. W. Yue, T. Xiang, W. F. Zhao, S. D. Sun and C. S. Zhao, *Sep. Sci. Technol.*, 2013, **48**, 1941-1953.
31. J. Ren, W. F. Zhao, C. Cheng, M. Zhou and C. S. Zhao, *Desalination*, 2011, **280**, 152-159.
32. C. S. Zhao, S. Q. Nie, M. Tang and S. D. Sun, *Prog. Polym. Sci.*, 2011, **36**, 1499-1520.
33. T. Xiang, L. R. Wang, L. Ma, Z. Y. Han, R. Wang, C. Cheng, Y. Xia, H. Qin and C. S. Zhao, *Sci. Rep.*, 2014, **4**, 4604.
34. W. F. Zhao, J. Y. Huang, B. H. Fang, S. Q. Nie, N. Yi, B. H. Su, H. F. Li and C. S. Zhao, *J. Membr. Sci.*, 2011, **369**, 258-266.
35. Z. Y. Han, C. Cheng, L. S. Zhang, C. D. Luo, C. X. Nie, J. Deng, T. Xiang and C. S. Zhao, *Desalination*, 2014, **349**, 80-93.

36. B. Yuan, Q. Chen, W. Q. Ding, P. S. Liu, S. S. Wu, S. C. Lin, J. Shen and Y. Gai, *ACS Appl. Mater. Interfaces*, 2012, **4**, 4031-4039.
37. F. J. Sun, C. M. Wu, Y. H. Wu and T. W. Xu, *J. Membr. Sci.*, 2014, **450**, 103-110.
38. H. Matsuyama, M. Nishiguchi and Y. Kitamura, *J. Appl. Polym. Sci.*, 2000, **77**, 776-783.
39. F. M. Cao, P. L. Bai, H. C. Li, Y. L. Ma, X. P. Deng and C. S. Zhao, *J. Hazard. Mater.*, 2009, **162**, 791-798.
40. E. Yuliwati and A. F. Ismail, *Desalination*, 2011, **273**, 226-234.
41. C. Feng, B. Shi, G. Li and Y. Wu, *J. Membr. Sci.*, 2004, **237**, 15-24.
42. X. Fan, Y. Su, X. Zhao, Y. Li, R. Zhang, J. Zhao, Z. Jiang, J. Zhu, Y. Ma and Y. Liu, *J. Membr. Sci.*, 2014, **464**, 100-109.
43. V. Vatanpour, S. S. Madaeni, R. Moradian, S. Zinadini and B. Astinchap, *Sep. Purif. Technol.*, 2012, **90**, 69-82.
44. J. H. Clint, *Curr. Opin. Colloid Interface Sci.*, 2001, **6**, 28-33.
45. T. Xiang, H. Fu, W. W. Yue, S. D. Sun and C. S. Zhao, *Sep. Sci. Technol.*, 2013, **48**, 1627-1635.
46. A. Nabe, E. Staude and G. Belfort, *J. Membr. Sci.*, 1997, **133**, 57-72.
47. J. Cho, G. Amy and J. Pellegrino, *J. Membr. Sci.*, 2000, **164**, 89-110.
48. P. Olsson, J. Sanchez, T. E. Mollnes and J. Riesenfeld, *J. Biomater. Sci., Polym. Ed.*, 2000, **11**, 1261-1273.
49. J. H. Lee, Y. M. Ju and D. M. Kim, *Biomaterials*, 2000, **21**, 683-691.
50. Z. Zhang, M. Zhang, S. F. Chen, T. A. Horbett, B. D. Ratner and S. Y. Jiang, *Biomaterials*, 2008, **29**, 4285-4291.
51. J. H. Seo, R. Matsuno, T. Konno, M. Takai and K. Ishihara, *Biomaterials*, 2008, **29**, 1367-1376.
52. N. Murthy, J. R. Robichaud, D. A. Tirrell, P. S. Stayton and A. S. Hoffman, *J. Controlled Release*, 1999, **61**, 137-143.
53. H. Nygren and M. Broberg, *J. Biomater. Sci., Polym. Ed.*, 1998, **9**, 817-831.
54. F. MacRitchie, *Adv. Protein Chem.*, 1978, **32**, 283-326.
55. W. C. Lin, T. Y. Liu and M. C. Yang, *Biomaterials*, 2004, **25**, 1947-1957.
56. Z. W. Wang, J. Z. Li and C. G. Ruan, *Thrombus and hemostasis: basic theory and clinic (2nd ed.)*, Shanghai Scientific and Technical Publishers: Shanghai, 1996.
57. D. W. Fu, B. Q. Han, W. Dong, Z. Yang, Y. Lv and W. S. Liu, *Biochem. Biophys. Res. Commun.*, 2011, **408**, 110-114.